Research Article

Received: 3 June 2021 Revised: 31 October 2021 Accepted article published: 5 November 2021 Published online in Wiley Online Library: 17 November 2021

(wileyonlinelibrary.com) DOI 10.1002/pi.6323

Resistance of glass fibre reinforced polyamide 6.6 materials to automotive cooling fluids: an analytical method for lifetime prediction

Konstantina Harrass,[a*] Sebastian Mauer[a] and Roumen Tsekov[b]

Abstract

Two types (with and without a hydrolysis stabilizer) of polyamide 6.6 (PA6.6) reinforced with 30% w/w glass fibres were examined against the influence of automotive cooling fluids, e.g. ethylene glycol aqueous solutions. The overall goal was to find a methodology to compare the performance of PA6.6 materials against the impacts of the hydrolysis environment. The stabilizer effect on the hydrolytic resistance of the materials was assessed using tensile tests according to ISO 527, and their strain-at-break values were evaluated in more detail. The degradation mechanism of both PA types was monitored by infrared spectroscopy and SEM. The material lifetime was described by the Arrhenius equation. The results show that the hydrolysis stabilizer operates effectively at low temperature but exhibits weak performance above 130 °C, which is explained by faster consumption of the stabilizing agent.

Supporting information may be found in the online version of this article.

Keywords: polyamide 6.6 reinforced with 30% w/w glass fibres; hydrolysis; tensile strain-at-break; Arrhenius equation; material lifetime

INTRODUCTION

Polyamides (PAs) are semicrystalline thermoplastics belonging to the group of engineering polymers. Due to the presence of carbon amide groups, PAs absorb water and other polar fluids,[1,2] which strongly affect their mechanical properties. As a result, the extensibility and toughness increase, while the elastic modulus and strength decrease. The incorporation of a reinforcing agent, e.g. glass fibres and other inorganic fillers, into the PA matrix generates a composite material which possesses better mechanical properties and thermal resistance than the neat material.[3–9] The amount and orientation of the glass fibres strongly influence the reinforcement effect.[10–13] Moreover, the mechanical properties of the composites depend on the properties of the fibres and matrix as well as on the fibre–matrix interactions acting as a link between them. Thus, the stress applied by an external load is transferred from the matrix to the fibres, where the mechanical energy can be absorbed.

During the past 30 years, PA6.6 reinforced with different amounts of glass fibres have been successfully employed in the automotive industry, especially for constructing parts used under the engine bonnet.[14] However, the temperature inside the engine compartment is extremely high, sometimes higher than 150 °C. Additionally, the simultaneous effect of humidity, oil and fuel must be considered, since all together they can significantly reduce the performance of the PA materials.[15] It is well known from the literature that, at specific experimental conditions such as elevated temperature, neutral or acidic water solutions,[16–24] humid atmosphere[25,26] and cooling fluids, e.g. ethylene glycol/water solutions,[12,13,15,27–30] PAs are able to undergo reversible hydrolysis. The macromolecules dissociate to products with lower molecular weight containing free reactive ends such as amine and carboxylic groups. As a result, the molar mass of the material is reduced significantly, which prompts catastrophic changes of the material properties.

In the case of a well-accepted material for construction components, the possible failure of a PA6.6 reinforced with 30% w/w glass fibres (PA6.6-GF30) due to hydrolysis limits its applicability. A foreseeable error of an engineering component around the engine section indicates an avoidable malfunction of the whole vehicle. Not only for cost reducing reasons but also because of potential accidents, a prediction method is needed for the lifetime evaluation of these PA6.6-GF30 materials. Because of the good mechanical and heat resistant properties, the substitution of PA6.6-GF30 with another material that has less sensitivity against hydrolysis is currently not a topic in applications of automotive engineering. To overcome these disadvantages, stabilizers

* *Correspondence to: K Harrass, Institute of Mechanical Engineering, Cologne University of Applied Sciences, Steinmuellerallee 1, 51643 Gummersbach, Germany. E-mail: konstantina.harrass@th-koeln.de*

a *Institute of Mechanical Engineering, Cologne University of Applied Sciences, Gummersbach, Germany*

b *Department of Physical Chemistry, University of Sofia, Sofia, Bulgaria*

against hydrolysis are incorporated into the material. The aim of this paper is the introduction of an applicable method for the lifetime prediction of PA6.6-GF30 materials stabilized by protecting additives.

The present research investigates the stability of two different types of PA6.6-GF30, with and without the presence of a stabilizer, on prolonged exposure to a cooling fluid at different temperatures. The resistance of the PA6.6.-GF30 materials against the hydrolytic surrounding is assessed by mechanical experiments. The main criterion 'strain-at-break' is identified to give an estimation for the mechanical performance of the material under tensile stress. Therefore, the material lifetime is defined until 50% reduction of this property. The Arrhenius equation is used to implement a prediction method for life cycle calculation.

Additionally, the materials are analysed through infrared spectroscopy in order to determine hydrolytic degradation and are qualitatively examined by SEM.

EXPERIMENTAL

Production of test bars by injection moulding process

Tensile test bars, made of PA6.6-GF30, were procured from Akro-Plastic GmbH (Niederzissen, Germany). Two different types of specimen of AKROMID® A3 GF30 were delivered: one containing a stabilizing agent against hydrolytic reactions and the other without stabilizer. These materials were denoted types 1 and 2, respectively. The production of the AKROMID® A3 GF30 materials was done at Akro-Plastic GmbH as follows. First, the dried PA was blended with the desired amounts of glass fibres and stabilizer, followed by compounding in a single screw extruder. Later, the compounds were granulated and processed with a 500 kN injection moulding machine to form A1 tensile bars, in accordance with ISO 527-1 and 2.[31,32] The injection moulding parameters were as follows: melt temperature 300 °C; mould temperature 100 °C; injection speed 26 cm^3 s^{-1}; injection/holding pressure 800 bar; cooling time 40 s.

The dry-as-moulded (DAM) test pieces were vacuum packed in aluminium bags directly after injection moulding to avoid absorption of water.

Storage of PA6.6-GF30 in autoclave vessels

Five test bars from each type of PA6.6-GF30 were weighed and then carefully fixed on the 1.5 mm diameter stainless steel holding wires (Fig. 1(a)), which ensured that the samples were locked in position inside the autoclave (Fig. 1(b)). Then, the stainless steel autoclave vessel, with a total volume of 300 mL, was filled with a cooling fluid (ethylene glycol/water 50% v/v mixture) until the tensile bars were completely covered (Fig. 1(c)). Finally, the autoclave vessel was pressure-sealed and placed in the oven for the required temperature and time (Fig. 1(d)).

As ethylene glycol material a commonly purchasable cooling fluid, namely Glysantin G34® (BASF SE, Ludwigshafen, Germany), was used. In each experiment distilled water was utilized for dilution of the cooling fluid, labelled 'water' in the following text.

Determination of the weight increase of PA6.6-GF30

Due to immersion of the samples in the cooling fluid at different temperatures (120, 135 and 150 °C) and times (24, 72, 168, 336, 504 and 1008 h), the weight of the PA6.6-GF30 material increases. Five test bars were stored at each temperature and time. In order to determine if a degradation process had already taken place inside the polymer material after 24 h, five specimens of both PA types were additionally included in the test series for each temperature. These five specimens were first dried after removal from the autoclave in a conventional oven (Heraeus, Thermo Scientific) for 48 h at 80 °C. Then, they were further dried in a vacuum oven (Reihe VO200, Memmert & Co. KG) for 48 h at 90 °C. The re-drying procedure was performed in order to restore the initial weight of the DAM samples and to estimate any change in the mechanical properties of the materials after immersing them in the fluid for 24 h. For all other specimens, the weight was determined exactly 30 min after the removal from the autoclave vessels by using a balance (XS204 Delta Range, Mettler Toledo). The following equation was used to calculate the weight increase:

$$\text{weight increase}\,(\%) = \frac{m_2 - m_1}{m_1} \times 100 \tag{1}$$

where m_2 is the weight of the test bar after storage in the cooling fluid and m_1 is the weight of the sample in the DAM state.

Mechanical properties

The quasi-static tensile test measurements were performed according to ISO 527-1 and 2 using a Zwick Roell Z010 tensile testing machine (Zwick GmbH & Co. KG, Ulm, Germany). All tensile test bars were examined at ambient temperature exactly 1 h after removal from the autoclave vessel, except that the DAM samples were tested immediately after removal from the aluminium bags. The Young's modulus E_t was determined using a testing speed of 1 mm min^{-1} by applying the equation

$$E_t = \frac{\sigma_2 - \sigma_1}{\varepsilon_2 - \varepsilon_1} \tag{2}$$

where $\varepsilon_2 = 0.25\%$ and $\varepsilon_1 = 0.05\%$ are the strain limits to ensure elastic behaviour, while σ_1 and σ_2 are the corresponding stress values according to ISO 527.

Using the same test pieces but a crosshead speed of 5 mm min^{-1}, the tensile stress-at-break σ_B and strain-at-break ε_B were evaluated, respectively, as

$$\sigma_B = \frac{F}{A} \qquad \varepsilon_B = \frac{\Delta L}{L_0} \times 100 \tag{3}$$

F is the force (measured in newtons) and A is the cross-section area (given in square millimetres) of the specimen from its initial width and thickness. In Eqn (3), ε_B is defined as a percentage, L_0 (mm) is the gauge length of the sample before the experiment and ΔL (mm) is the increase in gauge length of the tensile bar. The average values of E_t, σ_B and ε_B were calculated by testXpert II software, a proprietary analysis tool from Zwick. Each value presented in the Results corresponds to the average of five single measurements.

Attenuated total reflection infrared spectroscopy

Infrared spectra of PA6.6-GF30 were recorded via a Nicolet iS10 FTIR spectrometer (Thermo Fischer Scientific, Waltham, MA, USA) employing the attenuated total reflection (ATR) technique. A diamond ATR crystal was used for the measurements. For each temperature and time, a tensile bar was measured. The recorded IR spectra (wavenumber 4000–400 cm^{-1}) represent measurements of 32 scans.

Polym Int 2022; **71**: 724–733 wileyonlinelibrary.com/journal/pi
Polymer International published by John Wiley & Sons Ltd on behalf of Society of Industrial Chemistry.

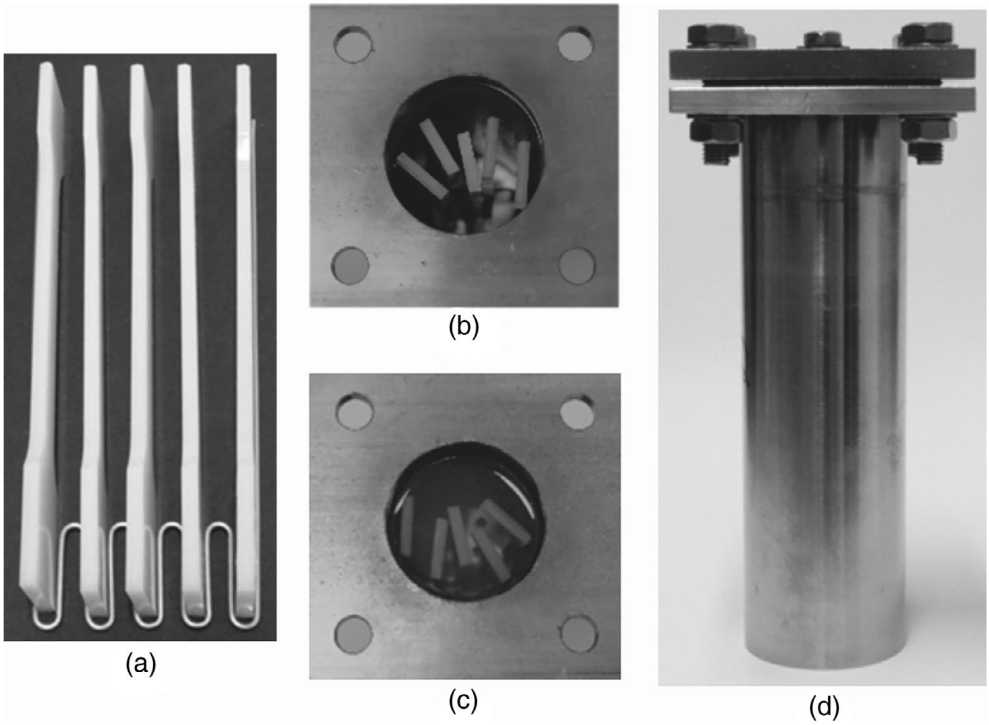

Figure 1. Storage of the test bars in an ethylene glycol/water mixture (50% v/v) in an autoclave vessel: (a) five test bars fixed on a holding wire; (b) view from the top inside the autoclave vessel with samples inserted; (c) view from the top inside the autoclave vessel filled with ethylene glycol/water; and (d) closed autoclave vessel.

Scanning electron microscopy (SEM)

The fracture surface of the test bars was observed after the tensile experiments using an SEM Leitz-AMR 1600T. Only typical DAM specimens and those stored for 42 days at three different temperatures were examined to show the maximum degree of degradation. The specimens were fixed on standard sample carriers equipped with conducting adhesive pads (C-Leit-Tabs, Plano GmbH, Wetzlar, Germany). Then, the surface was sputtered with gold for 2.5 min at $I = 15$ mA by using Polaron LTD E 5000 equipment (Quorum Technologies Ltd, Laughton, UK).

THEORETICAL CONSIDERATIONS

The Arrhenius equation presumes a linear dependence of the logarithm of the conditioning time at which a material property is reduced to 50% of its initial value on the reciprocal of temperature. The approach used in the present study is described in detail in ISO 2578.[33] The goal is to ascertain whether the Arrhenius equation fits the measured results well and to evaluate quantitatively the resistance of the PA6.6-GF30 materials against the influence of the cooling fluid. The measured properties of a material provide information about its capability to withstand the hydrolytic environment. Calculations according to the Arrhenius equation were utilized in order to verify whether it is applicable in the present study. Considering the storage experiments in a cooling fluid, the ageing process inside the polymers is described by the Arrhenius equation in accordance with ISO 2578:

$$L = A \exp\left(\frac{B}{T}\right) \tag{4}$$

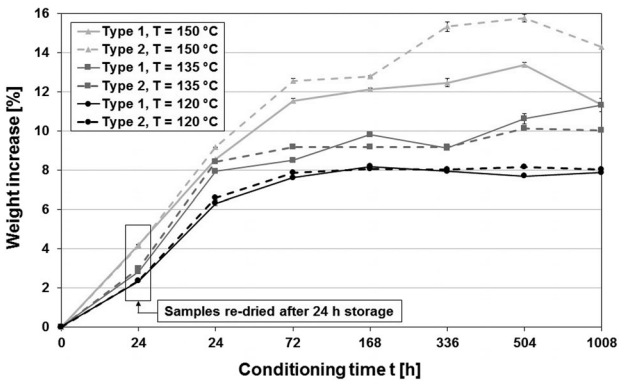

Figure 2. Weight increase of both PA6.6-GF30 types after storage in an ethylene glycol/water mixture (50% v/v) at different temperatures.

where the material lifetime L is the time in hours for 50% decrease of a material property, T is the absolute temperature and A and B are material-dependent constants.

RESULTS AND DISCUSSION

The results for the cooling fluid absorption in both types of PA6.6-GF30 at different temperatures and times are presented in Fig. 2. As expected, the increase of the temperature at which the tensile bars were stored causes a higher weight increase due to the fact that temperature accelerates the diffusion of the fluid inside the material. The maximal weight increase was detected for the specimens stored at a temperature of 150 °C.

Up to a conditioning treatment for 24 h, the weight increase is relatively fast in all samples but, after that, the weight increase continues to rise much more slowly. At temperatures of 120 and 135 °C, both types of PA6.6-GF30 reached maximal values of fluid saturation of approximately 8% and 10%, respectively, after storage for 168 h.

At a higher temperature of 150 °C, the maximal values for the weight increase (nearly 13% for type 1 and 16% for type 2) were achieved after storage for 504 h. The relatively strong decrease later at 1008 h can be explained by the fact that, at this high temperature and with prolonged conditioning treatment, the polymer starts to dissolve in the cooling fluid.[34] This process was so strong that an amount of dissolved material was detected as a precipitate on the bottom of the autoclave vessel after removing the tensile bars at the end of the experiment.

Furthermore, a re-drying procedure of the samples after 24 h storage was done. First, a standard oven with controlled temperature of 80 °C was used to re-dry the samples during 48 h, and then the process was continued using a vacuum oven (Memmert VO200) with applied low pressure of 5 mbar and also at 80 °C for the same time. The drying process at 80 °C is recommended by the raw materials manufacturer; however, the conditions were tightened in order to reach a fully dried situation inside the PA6.6-GF30 specimens.[35] Nevertheless, both re-drying procedures in series did not lead to restoration of the initial weight as measured for the DAM samples. The decrease of the weight of re-dried specimens reached only 50%. Due to the results observed, it can be assumed that only the water molecules diffuse outside and evaporate in the atmosphere while the ethylene glycol still remains inside the material. This assumption is supported by their different boiling points – 100 and 197 °C, respectively. The distinct boiling points result from the difference in vaporization energy of water and ethylene glycol, 44 and 60 kJ mol^{-1}, respectively.[36–38] However,

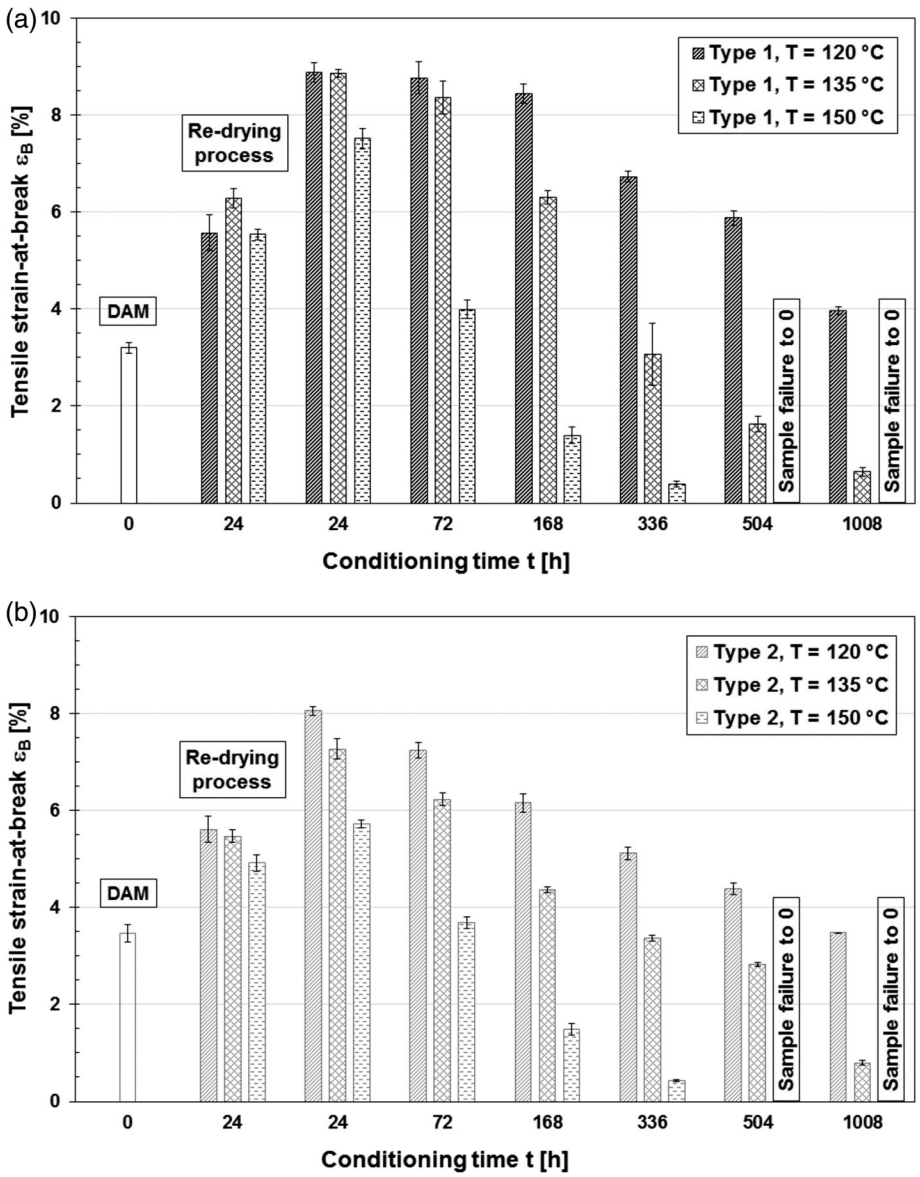

Figure 3. Comparison of the tensile strain-at-break of PA6.6-GF30 after storage in an ethylene glycol/water mixture (50% v/v) at different temperatures and times: (a) type 1 and (b) type 2.

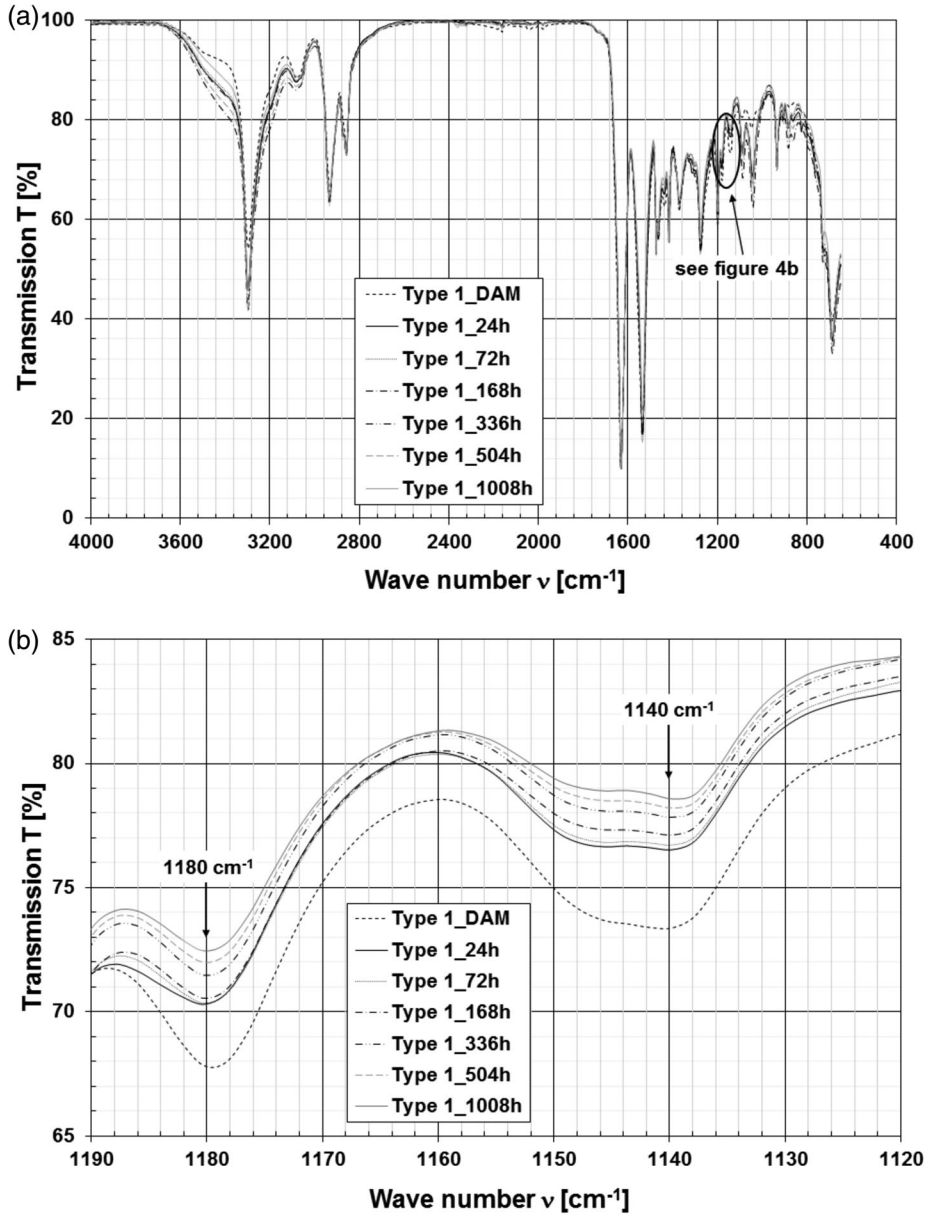

Figure 4. IR spectra of PA6.6-GF30, type 1, after conditioning at 120 °C at different times: (a) complete IR range and (b) IR range between 1190 and 1120 cm^{-1}.

inside the PA6.6 material the bonding energy of molecules absorbed to the amide group has to be overcome when they are abstracted. The bonding energy of water–amide bonds is around 30–35 kJ mol^{-1} as estimated by molecular modelling.[39,40] It can be supposed that the bonding energy of ethylene glycol to the amide group reaches an increased value, corresponding to its higher boiling point. The vapour pressure of pure ethylene glycol at 80 °C is 5 mbar, and it is 330 mbar for the 50 wt% aqueous ethylene glycol solution.[41] Therefore, the drying conditions should be enough for the total removal of cooling fluid agent. Despite that, the fact that the initial weight of DAM samples could not be reached can be explained only by strong interactive forces between the ethylene glycol and the amide groups in the polymer chains or hindered diffusion mechanisms for detachment of molecules. These interesting results arise alongside the main goal of the present research work. They were not followed up at this time but should be considered for research work in the future.

The mechanical properties of both types of PA6.6-GF30 were assessed with tensile test measurements. The tensile strain-at-break values were measured as criteria to evaluate the performance of PA6.6-GF30. This decision was because the fluids are mainly absorbed in amorphous regions of the PA materials.[42] The intermolecular and intramolecular van der Waals forces between the polymer chains and segments are much weaker compared to the analogues in the crystalline regions. Therefore, the penetration and diffusion of fluids into the material occurs predominately in the amorphous domains. Depolymerization and degradation processes can occur primarily to the PA chains, which are responsible for withstanding the tensile strain.

The results for ε_B for both types of PA6.6-GF30 are summarized in Figs 3(a) and 3(b). The tensile strain-at-break values for the PA

Polymer International published by John Wiley & Sons Ltd on behalf of Society of Industrial Chemistry.

material type 1 are shown in Fig. 3(a), while Fig. 3(b) shows the results of type 2 PA. The results in Figs 3(a) and 3(b) are given for different temperatures and conditioning times. Additionally, ε_B is presented in both diagrams for the DAM samples as well as for those obtained after re-drying (see also Fig. 2).

The PA6.6-GF30 type 1 specimens show nearly constant ε_B values after storing at conditioning temperatures 120 and 135 °C for 72 h (Fig. 3(a)), whereas the type 2 material exhibits a decrease caused by the degradation process (Fig. 3(b)). The strain-at-break of PA type 2 declines continuously with higher times for 120 and 135 °C and reaches approximately 4% and 1%, respectively, at 1008 h. On the other hand, ε_B of PA type 1 is slowly reduced with increasing times; however, at the longest duration of 1008 h the values show almost the same results as type 2. Nevertheless, 150 °C causes a decrease of ε_B values with rising conditioning times for both types of PA6.6-GF30. The highest temperature has such a strong effect on the PA material that the strain-at-break could not be measured due to total failure of the specimens at 504 and 1008 h.[43] The sample values were set to zero because the tensile tests could not be performed for these specimens (as labelled in both diagrams). The data for the samples of type 2 material after re-drying also show smaller values compared to those of type 1. This is not a large effect but it indicates that the start of the degradation process had already begun for type 2 after 24 h immersion time. The ε_B values of type 1 do not reduce to those measured for DAM samples because the total quantity of cooling fluid is not removed by re-drying, as was already discussed in the description for Fig. 2. Therefore, it can be assumed that the results for strain-at-break are summarized through effects of the remaining cooling fluid, i.e. mainly ethylene glycol, and influences of the beginning degradation process. In conclusion, it can be stated that the type 1 PA6.6.-GF30 material withstands immersion in the glycol/water mixture significantly better. In any case, temperature and conditioning time have a considerable effect on the materials' performance (i.e. on strain-at-break). The ε_B was consciously chosen as the failure criterion because a clear effect can be observed. In addition, also the stress-at-break (σ_B) values of the samples were measured. While the storage at 120 °C for the different conditioning times led to nearly no change of σ_B, the beginning of degradation can be observed at 135 °C for both types after 336 h. Only at 150 °C was the effect of hydrolysis recognizable at an early stage of 72 h. In the case of Young's modulus, the σ_B values are almost the same for all samples except for the ones that failed totally after storage. The reason is that Young's modulus is determined at small elongations according to ISO 527 and in this region the glass fibres primarily sustain the load applied.

In order to determine the degradation of the polymer material, IR spectroscopy analysis of both PA6.6-GF30 types was performed for all conditioning temperatures and times. Figure 4(a) displays exemplary IR spectra of PA type 1 for all times at an immersing temperature of 120 °C. Characteristic bands at 1180 and

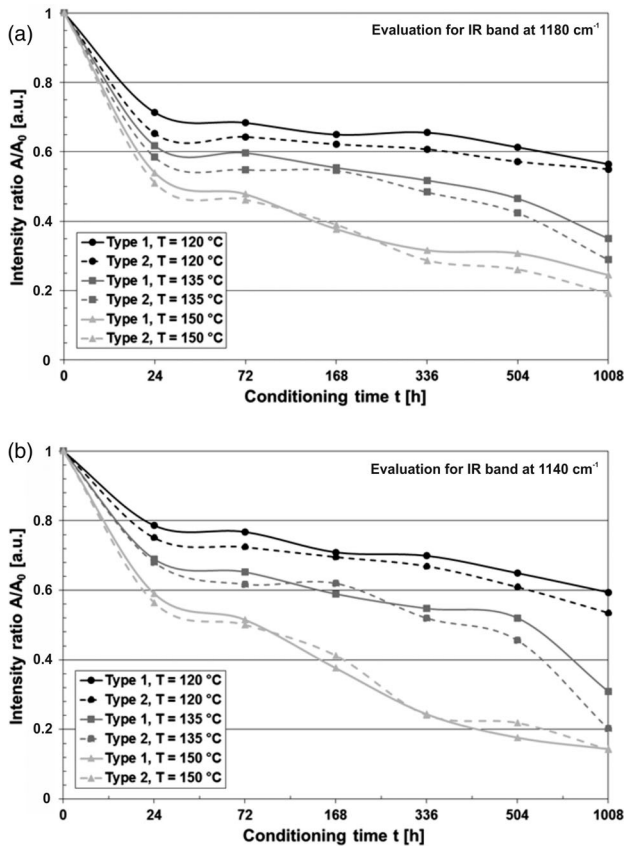

Figure 5. Changes in normalized integrated absorbance of both PA6.6-GF30 types as a function of the conditioning time: (a) IR band at 1180 cm^{-1} and (b) IR band at 1140 cm^{-1}.

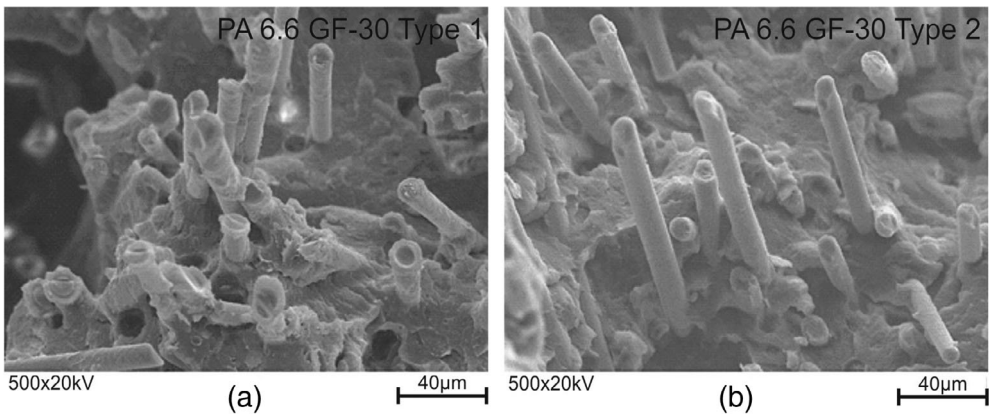

Figure 6. SEM micrographs of both PA6.6-GF30 types in the DAM state: (a) type 1, the fibres are strongly covered with the matrix; (b) type 2, less pronounced fibre–matrix interactions.

Polym Int 2022; **71**: 724–733

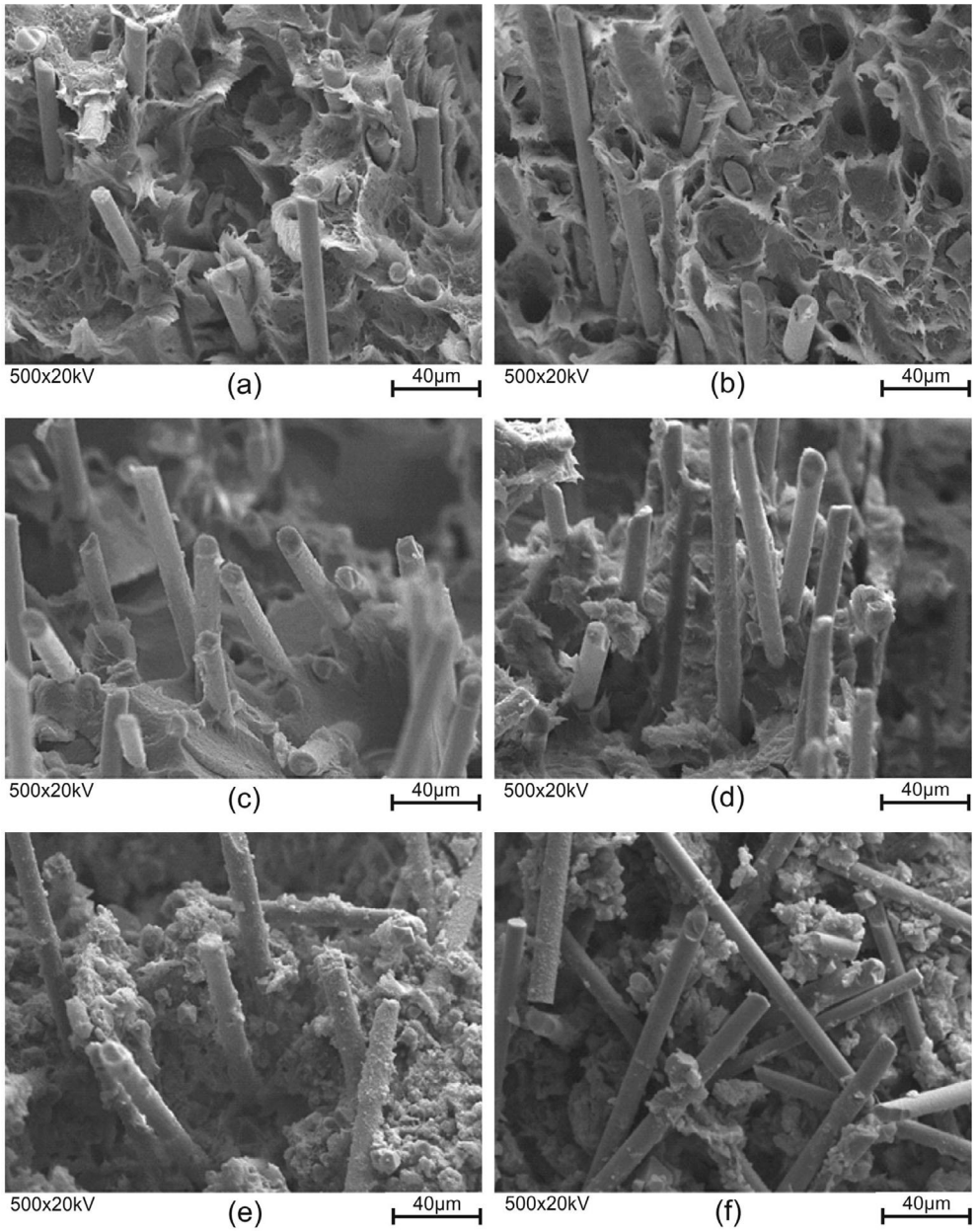

Figure 7. SEM micrographs of both PA6.6-GF30 types obtained for a conditioning time of 1008 h and different temperatures: (a), (b) for type 1 and 2, $T = 120$ °C; (c), (d) for type 1 and 2, $T = 135$ °C; (e), (f) for type 1 and 2, $T = 150$ °C.

1140 cm^{-1} originating from the methylene groups adjusted to nitrogen and the carbonyl groups, respectively, in the amorphous phase of the PA groups are observed.[42] To identify how the intensity of both IR bands changes with increase of the storage time, a magnified IR spectrum showing details is presented in Fig. 4(b). As expected, the longer conditioning times cause lower intensity of the IR bands at 1180 and 1140 cm^{-1}, i.e. the concentration of the amide groups decreases progressively due to a higher degree of polymer degradation. The observed tendency is similar for the other storage temperatures (135 and 150 °C), as shown in supporting information Figs S1 and S2.

In order to quantify the degradation process of both types of PA6.6-GF30, the areas under the characteristic IR bands at 1180 and 1140 cm^{-1} for all immersion temperatures and times were integrated and normalized against the internal reference bands, i.e. to the peak areas obtained for the DAM samples. The data of the integrated IR bands at 1180 cm^{-1} given in intensity ratio A/A_0 are shown in Fig. 5(a). Here, A represents the area of the sample after a specific conditioning time and temperature, and A_0 is the area for the initial DAM sample. For every temperature, a decrease is observed in the intensity ratio for both PA types against rising conditioning times. Also, the decrease of the intensity ratio against conditioning time increases with rising temperature. The intensity ratios of both PA types for 120 and 135 °C immersion temperature show a relatively smooth decrease, and PA type 1 exhibits higher values than those of type 2 for almost all sets. However, the ratios of both types at 150 °C reveal similar values, demonstrating identical rates of the degradation process at this temperature. Additionally, it is seen that the intensity ratios of the 24 h values already show a

Polymer International published by John Wiley & Sons Ltd on behalf of Society of Industrial Chemistry.

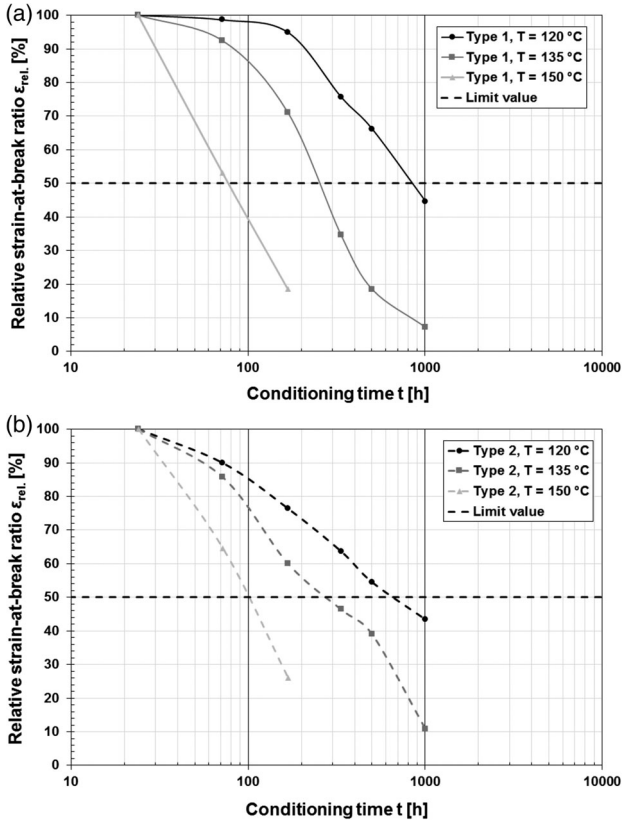

Figure 8. Determination of the time at which the tensile strain-at-break decreased to the 50% limit value for each temperature: (a) PA6.6-GF30, type 1, and (b) PA6.6-GF30, type 2.

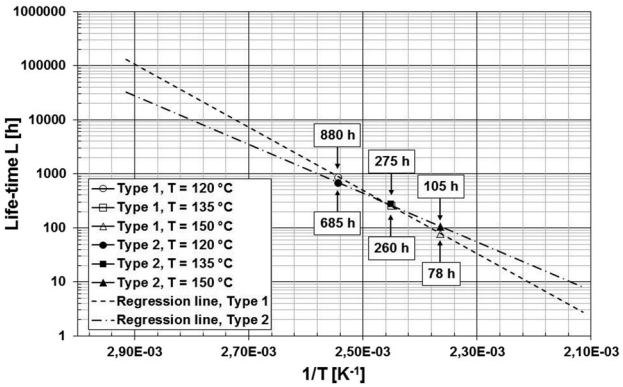

Figure 9. Comparison of the lifetimes for both PA6.6-GF30 types at three different temperatures: 120, 135 and 150 °C.

weak effect for all temperatures, which is proof of depolymerization at the beginning of storage.

The tendency identified by the IR band at 1180 cm^{-1} is analogous to the trend at 1140 cm^{-1} (see Fig. 5(b)). The intensity ratios for type 1 are higher compared to type 2. This is observed mainly for 120 and 135 °C, whilst at 150 °C the ratios for both PA types are nearly identical.

SEM analysis was used to determine the morphology of both types of PA6.6-GF30 in the DAM state as well as after immersion in the cooling fluid for 1008 h at 120, 135 and 150 °C. All SEM pictures were taken on the fractured surface of specimens after tensile experiments. As is usual for fracture patterns of glass fibre reinforced polymers, the effects of both broken and pulled-out fibres on matrix material are generally observable. Figure 6 compares the fracture surfaces of samples from both types in the DAM state. As presented in Fig. 6(a), the fibre–matrix interactions of type 1 are more pronounced since the glass fibres are strongly covered by the matrix. Thus, the load applied during the test can be easily transferred to the fibres because of their higher resistance to the external forces. In conclusion, it can be stated that the type 1 PA material exhibits better fracture performance than type 2 (Fig. 6(b)). As a reason, it can generally be explained as due to stronger fibre–matrix interactions. Both types originate from the same source; therefore, the glass fibres and matrix material are identical. The only difference is the presence of the stabilizing agent. This is why it can be assumed that the stabilizer also has an effect on the fibre–matrix interfaces of type 1. However, the tensile strain-at-break values of both types show similar results.

The fracture surfaces from the tensile experiments of both types of PA6.6-GF30, obtained after conditioning at the different temperatures for 1008 h, are presented in Figs 7(a)–(f). As expected, the absorption increase of the cooling fluid significantly changes the fracture surfaces: from a ductile (Figs 7(a) and (b)) to a brittle rupture (Figs 7(c) and 7(d)) or even to a completely damaged polymer matrix (Figs 7(e) and 7(f)).[44] The existence of moisture inside the composite material brings about a decrease of the tensile stress-at-break and tensile modulus, due to the lower transfer capability of stress between fibre–matrix interactions, as reported by Thomason.[12,13,27,28]

Furthermore, it can be assumed that the presence of the cooling fluid lowers the effect of the existing hydrogen bonds between the fibre and the moisture, and therefore it also reduces the effective van der Waals interactions between the fibres and the matrix. As a result, the matrix is no longer able to distribute the applied load through the total length of the adjacent glass fibres and the tensile strain-at-break increases. However, this behaviour is only observed for conditioning time up to 24 h. At immersion times of 72 h or longer and higher temperatures, the tensile strain-at-break starts to slowly decrease due to the hydrolytic degradation of the polymer chains. Due to the ongoing hydrolysis of the PA, the polymer chains become shorter, and thus they can absorb less deformational energy. Moreover, the comparison between the two PA materials leads to the conclusion that type 2 exhibits greater brittleness of the matrix with increasing temperature. The glass fibres are more exposed, which is evidence of a pull-out mechanism.[45]

The Arrhenius equation was applied to the tensile strain-at-break obtained for both PA6.6-GF30 types. Since the maximum ε_B values were obtained after conditioning the tensile bars for 24 h, they were considered as initial values to calculate a relative ratio by the normalization method. Following the standard approach from ISO 2578, the data obtained for tensile strain-at-break values at each immersing temperature (120, 135 and 150 °C) were plotted as the relative ratio $\varepsilon_{rel.}$ *versus* the conditioning times (Figs 8(a) and 8(b)).

As seen in Fig. 8, higher conditioning temperatures cause the limit values for both types of PA6.6-GF30 to be reached earlier. These results were expected since the higher temperatures bring about faster diffusion of the ethylene glycol and water molecules and, subsequently, quicker hydrolysis degradation of the polymer chains. Thus, the times to reach the limit value of 50% decrease are shorter. The lifetimes for both PA6.6-GF30 types in the

Polymer International published by John Wiley & Sons Ltd on behalf of Society of Industrial Chemistry.

temperature range from 70 to 200 °C were calculated by applying Eqn (4) and using the fitted constants. The regression lines used for the prediction were subsequently drawn and are shown in Fig. 9. The values determined for the lifetimes of both PA materials for desired temperatures are inserted on these regression lines. Based on the relationship from Eqn (4), the regression coefficients for both PA6.6-GF30 types were calculated and it is found that in all cases the experimental data follow the Arrhenius equation with $r \approx 1$.

By inspection of the regression lines in Fig. 9, it is concluded that PA6.6-GF30 type 1 exhibits a steeper slope than type 2. The conditioning temperature of 70 °C leads to a lifetime of 130 000 h for the PA sample type 1, whereas storing the type 2 material at the same temperature results in only 33 000 h lifetime, i.e. type 2 has just one quarter of the type 1 lifetime at 70 °C. However, the effect of the stabilizer incorporated in PA6.6-GF30 type 1 against hydrolysis seems to be negligible at temperatures above 130 °C, since the lifetime of type 1 stored above this temperature decreases significantly. Therefore, one can conclude that the hydrolysis stabilizer is consumed faster at higher temperatures. The faster diffusion of the cooling fluid inside the material must make a contribution but negligible impact of the hydrolysis stabilizer is evident at high temperatures.

CONCLUSIONS

The aim of the present study was to evaluate the effect of a cooling fluid (ethylene glycol/water 50% v/v mixture) on the mechanical properties of two different types of PA6.6-GF30, one with and the other without a hydrolysis stabilizer, designated as type 1 and type 2, respectively. The influence of several conditioning temperatures (120, 135 and 150 °C) and times (24, 72, 168, 336, 504 and 1008 h) was originally assessed on the weight increases of tensile bars produced as samples for testing purposes. It was revealed that the highest immersion temperature and the longest storage time brought about strong polymer degradation, which was also observed by the precipitation of decomposition products. Furthermore, a vacuum drying process of the specimens conditioned for 48 h at 90 °C did not result in the original DAM state being attained due to the strong physical interactions existing between the ethylene glycol and amide groups. The mechanical properties of specimens stored at the various conditioning temperatures and times were determined, and the change of tensile strain-at-break was considered. It was found that the PA6.6-GF30 samples enriched with hydrolysis stabilizer demonstrated better mechanical performance at lower conditioning temperatures; however, temperatures above 135 °C and longer storage times caused the opposite effect or even total failure of both types of material.

ATR IR spectroscopy was successfully applied to characterize the degradation behaviour of both PA6.6-GF30 types by evaluation of the peak intensities originating from characteristic groups at 1180 and 1140 cm^{-1}. The consequences of the fibre–matrix interactions were studied with the aid of SEM analysis which showed that type 1 material was better at withstanding the mechanical stress.

The Arrhenius equation was used to predict the lifetimes of both PA6.6-GF30 types. According to ISO 2578, the approach follows a 50% decrease of the initial value of the tensile strain-at-break as the limit for the useful life of a material. It was demonstrated that, at a temperature of 120 °C, PA6.6-GF30 type 1 exhibits a longer lifetime, whereas at 150 °C immersion temperature the PA material type 2 took a longer time to fail.

ACKNOWLEDGEMENTS

This paper is dedicated to the 80th Anniversary of Professor George S. Georgiev (Laboratory Water-Soluble Polymers, Polyelectrolytes and Biopolymers, Sofia University 'St Kliment Ohridski', Bulgaria). The authors gratefully acknowledge the Akro-Plastic GmbH (Niederzissen, Germany) for providing the materials, making it possible to perform the research. R. Tsekov is also grateful to the Bulgarian NSF for financial support under grant DGR 02/3.

SUPPORTING INFORMATION

Supporting information may be found in the online version of this article.

REFERENCES

1 Evstatiev M, Polyamides, in *Handbook of Thermoplastics*, Vol. **41**, ed. by Olabisi O. Marcel Dekker, New York, pp. 641–664 (1997).
2 Kuda-Malwathumullage CPS and Small GW, *J Appl Polym Sci* **131**: 40645–40653 (2014).
3 Thomason JL, *Compos Part A Appl Sci Manuf* **39**:1618–1624 (2008).
4 Thomason JL, *Compos Part A Appl Sci Manuf* **39**:1732–1738 (2008).
5 Kumar SS and Kanagaraj G, *Int J Polym Anal Charact* **21**:378–386 (2016).
6 Kumar SS and Kanagaraj G, *J Inorg Organomet Polym Mater* **26**:788–798 (2016).
7 Kumar SS and Kanagaraj G, *Bull Mater Sci* **39**:1467–1481 (2016).
8 Kumar SS and Kanagaraj G, *Arab J Sci Eng* **41**:4347–4357 (2016).
9 Kumar SS and Kanagaraj G, *J Polym Eng* **37**:547–557 (2017).
10 Akay M and Barkley D, *J Mater Sci* **26**:2731–2742 (1991).
11 Hassan A, Yahya R, Yahaya AH and Tahir RM, *J Reinf Plast Compos* **23**: 969–986 (2004).
12 Thomason JL, *Polym Compos* **27**:552–562 (2006).
13 Thomason JL, *Polym Compos* **28**:331–343 (2007).
14 Page IB, Polyamides as engineering thermoplastic materials, in *Rapra Review Reports*, Vol. **11**, No 1, Report 121. Rapra Technology Ltd, Shawbury (2000).
15 Bender KW, *Kunststoffe* **3**:66–70 (2010).
16 Heikens D, Hermans PH and Veldhoven HA, *Macromol Chem* **30**:154–168 (1959).
17 Williams A, *J Am Chem Soc* **98**:5645–5651 (1976).
18 Ogale AA, *J Appl Polym Sci* **29**:3947–3954 (1984).
19 Serpe G and Chaupart N, *Polymer* **38**:1911–1917 (1997).
20 Chaupart N, Serpe G and Verdu J, *Polymer* **39**:1375–1380 (1998).
21 Meyer A, Jones N, Lin Y and Kranbuehl D, *Macromolecules* **35**:2784–2798 (2002).
22 Jacques B, Werth M, Merdas I and Thominette F, *Polymer* **43**:6439–6447 (2002).
23 Merdas I, Thominette F and Verdu J, *Polym Degrad Stab* **79**:419–425 (2003).
24 Bernstein R, Derzon DK and Gillen KT, *Polym Degrad Stab* **88**:480–488 (2005).
25 Valentin D, Paray F and Guetta B, *J Mater Sci* **22**:46–56 (1987).
26 Bernstein R and Gillen KT, *Polym Degrad Stab* **95**:1471–1479 (2010).
27 Thomason JL, *Compos Part A Appl Sci Manuf* **40**:114–124 (2009).
28 Thomason JL, *Polym Compos* **28**:344–354 (2007).
29 Joacimi D, Grosser U and Krause F, *MTZ-Motortechnische Zeitschrift* **62**: 176–182 (2001).
30 Heyn J and Bonten C, *Kunststoffe* **11**:92–95 (2016).
31 ISO 527-1:2012. Plastics - Determination of tensile properties - Part 1: General principles.
32 ISO 527-2:2012. Plastics - Determination of tensile properties - Part 2: Test conditions for moulding and extrusion plastics.
33 ISO 2578:1998. Plastics - Determination of time-temperature limits after prolonged exposure to heat.
34 Geretschläger KJ and Wallner GM, *Polym Compos* **39**:997–1005 (2018).

35 Akro-Plastic (Ed.), *Productfilter AKROMID® A3 GF 30*. Available: https://akro-plastic.com/de/produktfilter/details/7751 [10 October 2021].
36 Barrett J, Inorganic chemistry in aqueous solution, in *Tutorial Chemistry Texts*, Vol. **21**. The Royal Society of Chemistry, Cambridge, pp. 1–12 (2003).
37 Petitjean M, Reyes-Perez E, Perez D, Mirabel P and Le Calve S, *J Chem Eng Data* **55**:852–855 (2010).
38 Al-Najjar H and Al-Sammerrai D, *J Chem Technol Biotechnol* **37**:145–152 (2007).
39 Hopmann RFW, *J Phys Chem* **78**:2341–2348 (1974).
40 Jorgensen WL and Swenson CJ, *J Am Chem Soc* **107**:1489–1496 (1985).
41 MEGlobal (Ed.), *Monoethylene Glycol (MEG) Technical Product Brochure*. Available: https://www.meglobal.biz/products-and-applications/product-literature/ [10 October 2021].
42 Goncalves ES, Poulsen L and Ogilby PR, *Polym Degrad Stab* **92**:1977–1985 (2007).
43 Lee J-Y and Kim K-J, *Molecules* **24**:755–765 (2019).
44 Ehrenstein G, Engel L, Klingele H and Schaper H, *Scanning Electron Microscopy of Plastics Failure*. Carl Hanser, Munich (2010).
45 Sato N, Kurauchi T, Sato S and Kamigaito O, *J Mater Sci* **19**:1145–1152 (1984).

